Original Article

Impact of plaque characteristics on percutaneous coronary intervention-related microvascular dysfunction: insights from angiographic microvascular resistance and intravascular ultrasound

Jianchang Xie[1]^, Ying He[2], Hao Ji[2], Qingqing Hu[2], Senjiang Chen[2], Beibei Gao[1], Jianmin Yang[1], Xiangbo Jin[1], Liang Zhou[1], Ningfu Wang[1], Xiaoshan Tong[1], Guoxin Tong[1], Jinyu Huang[1]

[1]Department of Cardiology, Affiliated Hangzhou First People's Hospital, Zhejiang University School of Medicine, Hangzhou, China; [2]The Fourth School of Clinical Medicine, Zhejiang Chinese Medical University, Hangzhou, China

Contributions: (I) Conception and design: J Xie, J Huang, G Tong; (II) Administrative support: J Huang, G Tong; (III) Provision of study materials or patients: G Tong, J Yang, N Wang, L Zhou, X Tong; (IV) Collection and assembly of data: Y He, H Ji, S Chen, Q Hu; (V) Data analysis and interpretation: J Xie, B Gao, X Jin; (VI) Manuscript writing: All authors; (VII) Final approval of manuscript: All authors.

Correspondence to: Jinyu Huang, MD; Guoxin Tong, MD. Department of Cardiology, Affiliated Hangzhou First People's Hospital, Zhejiang University School of Medicine, No. 261 Huansha Road, Shangcheng District, Hangzhou 310006, China. Email: hjyuo@163.com; sunnystewen@sina.com.

Background: The correlation between percutaneous coronary intervention (PCI)-related microvascular dysfunction (MVD) and plaque characteristics remains unclear. To investigate this correlation and its prognosis, we assessed changes in MVD by angiographic microvascular resistance (AMR) and intracoronary ultrasound scans after PCI.

Methods: We conducted a retrospective study that enrolled 250 patients with coronary artery disease between July 2016 and December 2018. We collected demographic characteristics, laboratory tests, coronary angiography (CAG) and intracoronary ultrasound findings. We calculated quantitative flow ratio (QFR) and AMR by CAG. The endpoint was vessel-oriented composite outcomes (VOCOs).

Results: After 47 exclusions, we divided 203 cases into a deteriorated group (n=139) and an improved group (n=64) based on AMR change after PCI. Compared with the improved group, the deteriorated group had smaller lumen area [3.03 (interquartile range, 2.20–3.91) *vs.* 3.55 mm^2 (interquartile range, 2.45–4.57), P=0.033], higher plaque burden [78.92% (interquartile range, 73.95–82.61%) *vs.* 71.93% (interquartile range, 62.70–77.51%), P<0.001], and higher proportion of lipidic components (13.86%±4.67% *vs.* 11.78%±4.41%, P=0.024). Of 186 patients who completed 4.81±1.55 years follow-up, 56 developed VOCOs. Receiver-operating characteristic (ROC) curve analysis showed post-PCI AMR and VOCOs correlation (area under the curve: 0.729, P<0.001). Multivariate regression analysis showed post-PCI AMR >285 mmHg·s/m correlated with adverse outcome (hazard ratio =4.350; 95% confidence interval: 1.95–9.703; P<0.001).

Conclusions: Intravascular ultrasound (IVUS) imaging and AMR revealed an association of post-PCI MVD with a smaller lumen area, more severe plaque burden, and a higher percentage of lipidic components. Post-PCI MVD was an independent risk factor for poor prognosis.

Keywords: Percutaneous coronary intervention (PCI); microvascular dysfunction (MVD); plaque characteristics; coronary angiography (CAG); intravascular ultrasound (IVUS)

^ ORCID: 0000-0001-8499-7626.

Submitted Apr 01, 2023. Accepted for publication Jul 10, 2023. Published online Aug 03, 2023.
doi: 10.21037/qims-23-414
View this article at: https://dx.doi.org/10.21037/qims-23-414

Introduction

Although percutaneous coronary intervention (PCI), in particular coronary stent implantation, successfully reverses myocardial ischemia caused by coronary stenosis, PCI-related microvascular dysfunction (MVD) seems to be important. PCI-related MVD is associated with a poor prognosis in patients with acute coronary syndrome (ACS) and those with stable angina pectoris (1,2). Mechanisms of MVD include mechanical plugging secondary to distal embolization from the epicardial coronary arteries, external compression by edematous tissue, *in situ* thrombosis, vasospasm, activation of inflammatory cascades with leukocyte stasis and extravasation, and reperfusion injury (3). The plaque characteristics of target lesions may play an important role in causing MVD during PCI (4).

In clinical practice, marked slow flow or no reflow are common complications of intervention for ACS. However, most PCI-related MVD manifests as normal flow and requires an index of microvascular resistance (IMR), cardiac magnetic resonance imaging, or cardiac nuclear scanning. There has been little research on the extent to which plaque characteristics affect coronary microvascular outcomes. Given its complexity and high cost, measurement of the IMR is difficult to implement widely, although it is endorsed in the current guidelines. The quantitative flow ratio (QFR) is a novel coronary angiography (CAG)-based coronary physiology approach that has been widely recognized for its ability to accurately identify coronary ischemia and has a test efficacy comparable with that of the pressure wire-based fractional flow reserve (FFR) (5). CAG-based microvascular function examinations have also developed in parallel with the progress made in CAG-based assessment of coronary function and show good agreement with IMR (6-9). Angiographic microvascular resistance (AMR), QFR-derived IMR, appears to be more rapid to perform, more convenient, and less expensive, allowing further research into PCI-related MVD (9). The aim of this study was to assess the relevance of coronary plaque to PCI-related MVD and the prognosis by assessing changes in MVD seen on AMR and intravascular ultrasound (IVUS) after PCI.

Methods

Population

A total of 250 patients diagnosed with previously untreated coronary heart disease in the Department of Cardiology, Affiliated Hangzhou First People's Hospital, Zhejiang University School of Medicine between July 2016 and December 2018 were retrospectively screened. The study was conducted in accordance with the Declaration of Helsinki (as revised in 2013). The study was approved by ethics board of Affiliated Hangzhou First People's Hospital, Zhejiang University School of Medicine, and individual consent for this retrospective analysis was waived. All patients with successful stenting and complete information available on IVUS and QFR analysis were included. The following exclusion criteria were applied: incomplete clinical or follow-up data; poor-quality IVUS or CAG images; a total occlusive lesion; coronary thrombolysis; marked slow flow or no reflow after PCI [thrombolysis in myocardial infarction (TIMI) grade <3]; culprit lesions that were not *de novo*, such as in-stent restenosis; heart failure (ejection fraction <50%); and stage 5 chronic kidney disease.

PCI procedure

According to routine practice, all patients received adequate antiplatelet therapy before PCI. Unfractionated heparin (100–120 μg/kg) was administered to maintain an activated clotting time of >300 s throughout the procedure. Standard selective CAG was performed using 5-French catheters. The PCI strategies were based on information from the patient history, CAG, and IVUS. Drug-eluting stents were implanted after adequate predilatation of the target lesion. The ratio of stent diameter to symmetric vessel diameter is 1.0–1.1:1, and the balloon inflation pressure is 12–16 atm for at least 10 s. After implantation, the stents were fully dilated using a noncompliant balloon, and the minimum lumen area was confirmed to be not less than 80% of the average reference vessel area as assessed by IVUS. The filter devices were not used in this study.

IVUS procedure

An iLab system, along with a 40-MHz mechanical IVUS

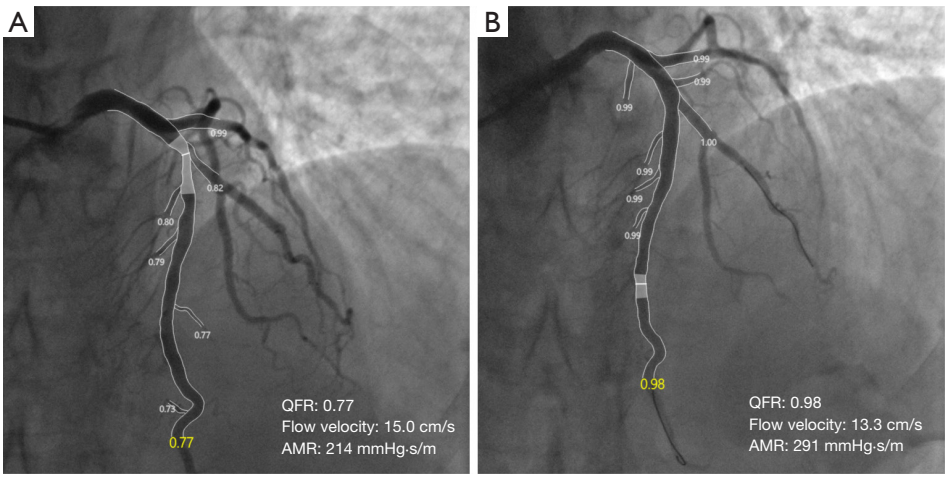

Figure 1 Examples of QFR and AMR analysis. CAG showed a stenosis in the proximal left anterior descending, and QFR was calculated as 0.77, flow velocity was 15.0 cm/s, AMR was calculated as 214 mmHg·s/m (A). After stent implantation, QFR was calculated as 0.98, flow velocity was 13.3 cm/s, and AMR was calculated as 291 mmHg·s/m (B). QFR, quantitative flow ratio; AMR, angiographic microvascular resistance; CAG, coronary angiography.

catheter-tip transducer from Boston Scientific (Natick, MA, USA), was used to acquire IVUS data. The catheter-tip transducer was rotating at a speed of 1,800 rpm during imaging. IVUS scans and plaque analyses were performed before the stent implantation and balloon dilatation. Automatic pullback at a rate of 0.5 mm/s was used during imaging while the catheter was pushed beyond the target lesion. All images were assigned with random study ID numbers based on a pre-determined list and collected on CD-ROMs for the purpose of offline analysis. Two experienced analysts who were blinded to the angiographic findings and baseline clinical and lesion characteristics analyzed the gray-scale IVUS images. The analysis was carried out using the QIvus (iMap Basic Viewer 3.0, Medis Medical Imaging Systems BV, Leiden, The Netherlands) software.

For each culprit lesion, the cross-sectional area (CSA) exhibiting maximum plaque burden was used as representative CSA. This was done by manually tracing the lumen and external elastic membrane (EEM). Using the traced CSA, the plaque burden was computed as a quotient of plaque CSA (EEM-lumen CSA) and EEM. Lumen and vessel volumes were obtained by summing up the lumen and EEM areas, respectively, in each of the measured images. The total atheroma volume was calculated as the difference between vessel volume and lumen volume. The percentage atheroma volume was determined as (total atheroma volume/vessel volume) × 100%.

Plaque was analyzed using the iMap software, which categorized it into four different tissue components and generated color images. Fibrous plaque was represented by the color green, lipidic plaque by yellow, necrotic plaque by pink, and calcified plaque by blue.

Quantitative CAG measurements and analysis of QFR and AMR

To ensure the quality of the quantitative CAG and QFR analyses, two high-quality CAG projections at least 25° apart are required after PCI, and these analyses are performed by two experienced technicians using AngioPlus software (Pulse Medical Imaging Technology, Shanghai, China). The contrast flow model, which incorporates contrast flow velocity based on modified TIMI frame counts, was used to calculate the QFR. AMR was then calculated using the AngioPlus system based on contrast flow velocity and the QFR (9). ΔQFR, ΔAMR, and Δflow velocity were calculated as the difference between the parameters before and after stenting. Deterioration of microvascular resistance was defined as an increase in AMR after stenting (*Figure 1*).

Follow-up and endpoints

The endpoint was the rate of vessel-oriented composite outcomes (VOCOs), which consisted of vessel-related ischemia-driven revascularization, vessel-related myocardial infarction, and cardiac death. Clinical follow-up was performed

by review of medical records and telephone contact every 6 months. Patients were followed up for 5–7 years.

Statistical analysis

Continuous variables are presented as the mean ± standard deviation or as the median (interquartile range) according to their distribution and were compared using the two-tailed unpaired Student's *t*-test or the Mann-Whitney test. The ability of microvascular resistance post-PCI to predict VOCOs was tested using receiver-operating characteristic (ROC) curve analysis. The Cox proportional hazards model was used to calculate hazard ratios (HRs) and 95% confidence intervals (CIs) for between-group comparisons of clinical outcomes. The cumulative incidence of VOCOs is presented as a Kaplan-Meier estimate and compared using the log-rank test. All statistical analyses were performed using SPSS version 26.0 for Windows (IBM Corp., Armonk, NY, USA). All probability values were two-tailed, and P values <0.05 were considered statistically significant.

Results

Baseline and coronary angiographic characteristics

Forty-seven of the 250 patients enrolled in the study were excluded because of unsatisfactory coronary angiographic images (n=14), poor-quality intracoronary ultrasound images (n=20), markedly slow postoperative flow (TIMI grade <3; n=5), and heart failure (ejection fraction <50%; n=8), leaving 203 patients for inclusion in the study. The group with increased AMR after stenting (the deteriorated group) consisted of 139 patients and the group with decreased AMR (the improved group) consisted of 64 patients (*Table 1*).

Effect of PCI on microvascular function

Given that there was a correlation between the calculated AMR and QFR and that there were significant differences in QFR, AMR, and flow velocity in the pre-procedure baseline data, we performed propensity score matching (PSM) for these three variables and successfully matched 50 pairs of cases for comparison of the data between the two groups. Both before and after matching, the flow velocity after PCI was significantly slower in the deteriorated group than in the improved group. Analysis of the IVUS data showed that the deteriorated group had a significantly smaller lumen CSA [3.03 (2.20–3.91) *vs.* 3.55 mm^2 (2.45–4.57), P=0.033 after PSM], a significantly higher plaque burden [78.92% (73.95–82.61%) *vs.* 71.93% (62.70–77.51%), P<0.001 after PSM], and a significantly higher proportion of lipidic components (13.86%±4.67% *vs.* 11.78%±4.41%, P=0.024

Table 1 Characteristics of patients with microvascular function after PCI, by deteriorated and improved

Patient characteristics	Total (n=203)	Original cohort			Propensity score† matched cohort		
		Deteriorated group (n=139)	Improved group (n=64)	P value	Deteriorated group (n=50)	Improved group (n=50)	P value
Male	135 (66.5)	88 (63.3)	47 (73.4)	0.2	34 (68.0)	38 (76.0)	0.504
Age (years)	67.03±10.99	67.69±10.83	65.61±11.27	0.211	66.69±10.77	66.38±11.51	0.795
Hypertension	136 (67.0)	93 (66.9)	43 (67.2)	1	33 (66.0)	35 (70.0)	0.830
Diabetes mellitus	54 (26.6)	38 (27.3)	16 (25.0)	0.864	12 (24.0)	13 (26.0)	1.000
Current smokers	83 (40.9)	53 (38.1)	30 (46.9)	0.283	25 (50.0)	25 (50.0)	1.000
ACS	123 (60.6)	94 (67.6)	29 (45.3)	0.003	36 (72.0)	28 (56.0)	0.063
BMI (kg/m^2)	23.63±3.16	23.58±3.15	23.71±3.20	0.783	24.55±2.75	23.48±3.10	0.071
Total cholesterol (mmol/L)	3.98±1.09	3.94±1.07	4.07±1.12	0.434	3.98±1.03	4.08±1.00	0.604
LDL cholesterol (mmol/L)	2.25±0.88	2.21±0.89	2.34±0.87	0.713	2.26±0.89	2.32±0.83	0.760
HDL cholesterol (mmol/L)	1.05±0.48	1.06±0.55	1.04±0.25	0.324	1.01±0.22	1.03±0.27	0.649
Triglyceride (mmol/L)	1.59±0.89	1.53±0.81	1.74±1.03	0.115	1.65±0.94	1.68±0.8	0.839
C-reactive protein (mg/L)	4.0 (3.0–5.0)	4.0 (3.0–5.0)	4.0 (3.0–5.75)	0.500	4.0 (3.0–5.0)	4.0 (3.0–6.0)	0.517
eGFR-CKD-EPI ($mL/min/1.73\ m^2$)	73.90±15.61	72.54±15.39	76.85±15.78	0.068	73.93±14.91	75.54±16.21	0.607

Table 1 *(continued)*

Table 1 *(continued)*

Patient characteristics	Total (n=203)	Original cohort			Propensity score† matched cohort		
		Deteriorated group (n=139)	Improved group (n=64)	P value	Deteriorated group (n=50)	Improved group (n=50)	P value
HbA1c (%)	5.60 (5.30–6.60)	5.70 (5.30–6.60)	5.50 (5.10–6.53)	0.084	5.60 (5.30–6.45)	5.55 (5.10–6.68)	0.548
Diameter stenosis‡	72.66±10.54	73.71±10.88	70.38±9.46	0.036	72.68±10.33	70.94±8.96	0.370
Target lumen							
LAD	122 (60.1)	85 (61.2)	37 (57.8)	0.485	29 (58.0)	32 (64.0)	0.165
LCX	30 (14.8)	19 (13.7)	11 (17.2)		9 (18.0)	5 (10.0)	
RCA	37 (18.2)	24 (17.3)	13 (20.3)		11 (22.0)	9 (18.0)	
LM-LAD	10 (4.9)	9 (6.5)	1 (1.6)		0 (0.0)	4 (8.0)	
LM-LCX	4 (2.0)	2 (1.4)	2 (3.1)		1 (2.0)	0 (0.0)	
Pre-PCI							
QFR	0.78 (0.68–0.86)	0.76 (0.60–0.83)	0.84 (0.75–0.90)	<0.001	0.79 (0.71–0.86)	0.82 (0.73–0.87)	0.454
Flow velocity (cm/s)	14.75 (11.80–18.50)	16.18 (12.80–19.53)	11.80 (10.78–14.61)	<0.001	12.95 (11.50–15.85)	12.59 (10.98–15.82)	0.694
AMR (mmHg·s/m)	208.44±59.11	188.26±53.76	252.26±44.97	<0.001	237.88±37.76	232.59±48.10	0.685
Post-PCI							
QFR	0.95 (0.92–0.97)	0.95 (0.92–0.98)	0.95 (0.92–0.97)	0.646	0.96 (0.92–0.98)	0.94 (0.91–0.96)	0.126
Flow velocity (cm/s)	15.20 (12.00–18.10)	13.58 (11.20–16.60)	18.20 (14.83–24.59)	<0.001	12.35 (10.68–15.18)	19.26 (16.19–27.18)	<0.001
AMR (mmHg·s/m)	265.43±56.19	282.33±53.25	238.73±43.75	<0.001	301.38±55.53	216.61±40.07	<0.001
IVUS							
Segment length (mm)	25.00 (15.70–36.80)	26.0 (15.80–36.0)	23.05 (15.00–38.38)	0.598	25.75 (15.00–38.68)	27.0 (15.81–39.20)	0.866
Lumen CSA (mm^2)	3.11 (2.30–4.06)	2.76 (2.22–3.70)	3.74 (2.53–4.82)	<0.001	3.03 (2.20–3.91)	3.55 (2.45–4.57)	0.033
EEM CSA (mm^2)	13.45 (10.89–15.67)	14.07 (10.93–17.19)	12.87 (10.41–15.95)	0.156	14.02 (11.43–18.35)	12.27 (10.05–15.51)	0.052
Plaque burden (%)	77.46 (70.87–81.83)	79.70 (74.30–83.02)	70.72 (62.11–77.26)	<0.001	78.92 (73.95–82.61)	71.93 (62.70–77.51)	<0.001
Fibrotic area (%)	55.06±20.10	53.89±20.39	57.59±19.37	0.224	56.34±20.37	57.06±19.60	0.857
Lipidic area (%)	13.00±4.79	13.58±4.89	11.72±4.32	0.010	13.86±4.67	11.78±4.41	0.024
Necrotic area (%)	30.45±17.01	30.99±17.21	29.30±16.63	0.512	28.56±17.30	29.80±17.00	0.719
Calcified area (%)	1.52±1.92	1.54±1.19	1.48±1.07	0.731	1.16±1.43	1.48±2.02	0.364
Lumen volume (mm^3)	127.54 (72.49–220.39)	128.39 (73.13–210.22)	124.87 (70.19–243.63)	0.982	139.47 (80.47–217.43)	126.80 (69.38–251.08)	0.679
Vessel volume (mm^3)	326.43 (199.26–531.60)	342.86 (213.46–521.64)	292.75 (176.94–561.13)	0.297	373.77 (229.08–524,13)	312.10 (175.99–598.03)	0.412
PAV (%)	60.88 (52.33–70.08)	61.33 (53.62–71.12)	58.09 (50.07–68.01)	0.041	60.57 (51.57–70.75)	61.06 (50.54–68.12)	0.267
Fibrotic volume (%)	60.63±12.37	59.49±13.10	63.10±10.26	0.053	61.19±12.38	62.12±10.02	0.682
Lipidic volume (%)	12.00±3.51	12.30±3.47	11.36±3.55	0.076	12.33±3.64	11.21±3.30	0.109
Necrotic volume (%)	24.72±10.25	25.61±10.88	22.78±8.47	0.068	24.16±10.01	23.79±8.30	0.839
Calcified volume (%)	2.67±2.24	2.61±2.14	2.78±2.06	0.593	2.32±1.86	2.90±2.47	0.190

Data are expressed as mean ± standard deviation or median (interquartile range) or number (%). †, propensity score was matched by pre-PCI QFR, flow velocity, and AMR; ‡, diameter stenosis was examined by quantitative coronary angiography. PCI, percutaneous coronary intervention; ACS, acute coronary syndrome; BMI, body mass index; LDL, low density lipoprotein; HDL, high density lipoprotein; eGFR-CKD-EPI, estimated glomerular filtration rate-chronic kidney disease-epidemiology collaboration equation; LAD, left anterior descending; LCX, left circumflex; RCA, right coronary artery; LM, left main; QFR, quantitative flow ratio; AMR, angiographic microvascular resistance; IVUS, intravascular ultrasound; CSA, cross sectional area; EEM, external elastic membrane; PAV, percent atheroma volume.

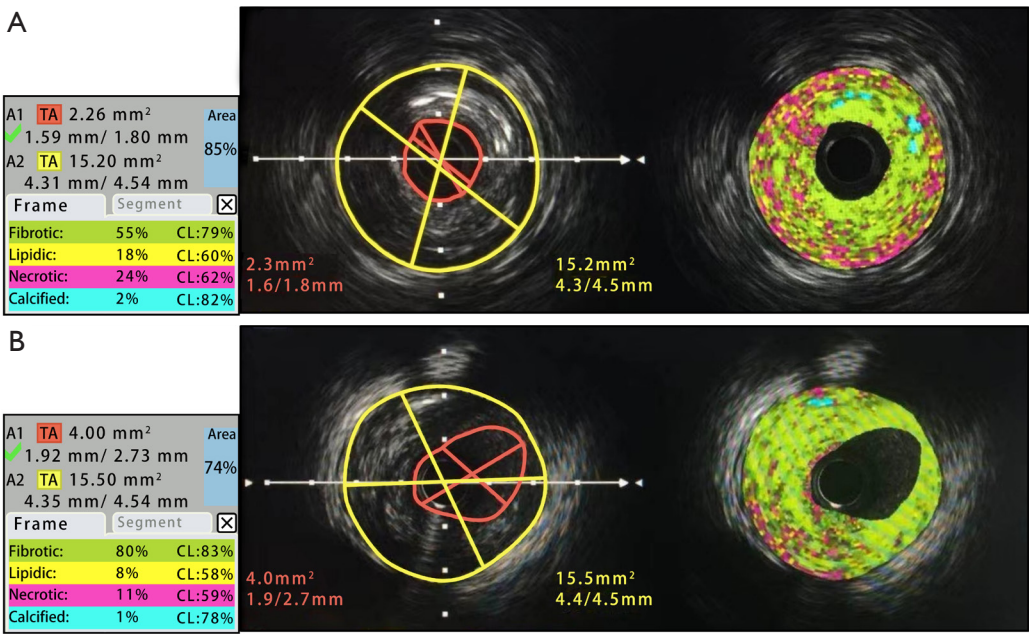

Figure 2 Examples of intracoronary ultrasound analysis of a plaque. A representative IVUS image of microvascular deterioration after PCI. EEM was 15.20 mm^2, lumen CSA was 2.26 mm^2, and plaque burden was 85% of (EEM-lumen CSA)/EEM. In terms of plaque composition, fibrotic: 55%, lipidic: 18%, necrotic: 24%, and calcified: 2% representatively (A). A representative IVUS image of microvascular improved after PCI. EEM was 15.50 mm^2, lumen CSA was 4.0 mm^2, and plaque burden was 74%. The ratio of plaque was fibrotic: 80%, lipidic: 8%, necrotic: 11%, and calcified: 1% representatively (B). TA, trace areas; CL, confidence level; IVUS, intracoronary ultrasound; PCI percutaneous coronary intervention; EEM external elastic membrane; CSA cross sectional area.

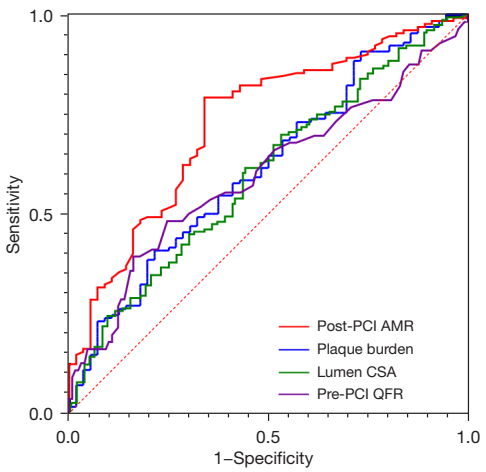

Figure 3 Receiver-operating characteristic curve analysis. Post-PCI AMR, plaque burden, lumen CSA, pre-PCI QFR and VOCOs were correlated with area under the curve of 0.729, 0.617, 0.606 and 0.589, respectively, with P values of <0.001, 0.012, 0.022, and 0.033. PCI, percutaneous coronary intervention; AMR, angiographic microvascular resistance; CSA, cross-sectional area; PCI, percutaneous coronary intervention; QFR, quantitative flow ratio; VOCOs, vessel-oriented composite outcomes.

after PSM) when compared with the improved group (*Table 1*, *Figure 2*).

Correlation analysis between MVD and the prognosis

Seventeen patients were lost to follow-up, leaving 186 patients who completed a mean follow-up of 4.81±1.55 years, during which 56 patients developed VOCOs.

In the ROC curve analysis for correlation with VOCOs, the area under the curve (AUC) was 0.729 for post-PCI AMR (P<0.001), 0.617 for plaque burden (P=0.012), 0.606 for lumen CSA (P=0.022), and 0.589 for pre-PCI QFR (P=0.033) (*Figure 3*, *Table 2*). When the post-PCI AMR was >285 mmHg·s/m, the sensitivity for predicting the occurrence of VOCOs was 79.23% and the specificity was 66.07%.

Univariate Cox proportional hazard analyses suggested associations between a post-PCI AMR >285 mmHg·s/m, pre-PCI QFR, post-PCI flow velocity, plaque burden, deterioration of microvascular function during PCI, ACS, and adverse outcomes. Collinearity diagnostics revealed

multicollinearity between post-PCI AMR and other variables and was therefore excluded from the multivariate Cox regression model. Multivariate Cox proportional hazard analyses showed a significant correlation between a post-PCI AMR >285 mmHg·s/m and adverse outcomes (HR =4.350; 95% CI: 1.95–9.703; P<0.001; *Table 3*). When using an AMR cutoff of 285 mmHg·s/m derived from the ROC curve for predicting VOCOs, the cumulative incidence of VOCOs was significantly higher in patients with an AMR >285 mmHg·s/m than in those with an AMR ≤285 mmHg·s/m (P<0.001) (*Figure 4*).

Discussion

In this study, we assessed coronary microvascular function using CAG-based IMR in combination with IVUS-related plaque characteristics to analyze the effect of PCI on microvascular function and the prognosis. The main findings were as follows: first, deteriorated microvascular function after PCI was common (139/203, 68.47%); second, there was a correlation of post-PCI MVD with a smaller luminal CSA, more severe plaque burden, and higher percentage of lipidic components; and third, post-PCI MVD was an independent risk factor for a poor prognosis.

The presence of MVD after PCI is common and its association with a poor prognosis is well established, especially in patients with ACS, in whom no reflow is a challenge in the catheterization laboratory. Our study found that a certain percentage of MVD was present even when post-PCI TIMI flow reached grade 3. According to a previous study, the best cut-off AMR value for determination of IMR ≥25 was 250 mmHg·s/m (9), and in our present study, the proportion with AMR >250 mmHg·s/m was 54.68% (111/203). A previous multicenter study with a 4-year follow-up period found that an IMR >21.6 after PCI in patients with stable coronary artery disease was associated with a poor prognosis (2). Another study identified an IMR >40 post-PCI to be an independent risk factor for a poor prognosis in patients with ST-segment elevation myocardial infarction (10). The high cost, complexity, and safety of the pressure wire limit its widespread use for assessment of microvascular function after PCI.

In recent years, the CAG-related FFR has shown very good agreement with wire-related FFR (11). In particular, several recently published studies have provided an evidence base for use of CAG-FFR to guide PCI (12,13). Based on the CAG-FFR, the studies of CAG-IMR verified the

Table 2 ROC curve analysis for correlation with VOCOs

Associated factor	AUC	95% CI	P value
Post-PCI AMR	0.729	0.651–0.808	<0.001
Plaque burden	0.617	0.529–0.704	0.012
Lumen CSA	0.606	0.519–0.684	0.022
Pre-PCI QFR	0.589	0.504–0.694	0.033

ROC, receiver-operating characteristic; VOCOs, vessel-oriented composite outcomes; AUC, area under the curve; CI, confidence interval; PCI, percutaneous coronary intervention; AMR, angiographic microvascular resistance; CSA, cross sectional area; QFR, quantitative flow ratio.

Table 3 Cox proportional hazard analysis of prognostic correlates

Associated factor	Univariate analysis		Multivariate analysis	
	HR (95% CI)	P value	HR (95% CI)	P value
Post-PCI AMR	1.009 (1.006–1.013)	<0.001	Not selected	
Post-PCI AMR >285 mmHg·s/m	5.482 (3.137–9.580)	<0.001	4.350 (1.95–9.703)	<0.001
Pre PCI-QFR	0.111 (0.026–0.437)	0.004	0.217 (0.046–1.017)	0.053
Post-PCI flow velocity (cm/s)	0.853 (0.795–0.915)	<0.001	0.983 (0.895–1.079)	0.720
Plaque burden (%)	1.038 (1.005–1.072)	0.022	1.004 (0.960–1.050)	0.852
Lumen CSA (mm^2)	0.807 (0.653–0.999)	0.049	0.911 (0.701–1.184)	0.485
Deterioration of microvascular function during PCI	3.590 (1.696–7.599)	0.001	0.848 (0.325–2.213)	0.737
ACS	1.947 (1.063–3.567)	0.031	0.994 (0.539–1.834)	0.985

HR, hazard ratio; CI, confidence interval; PCI, percutaneous coronary intervention; AMR, angiographic microvascular resistance; QFR, quantitative flow ratio; CSA, cross sectional area; ACS, acute coronary syndrome.

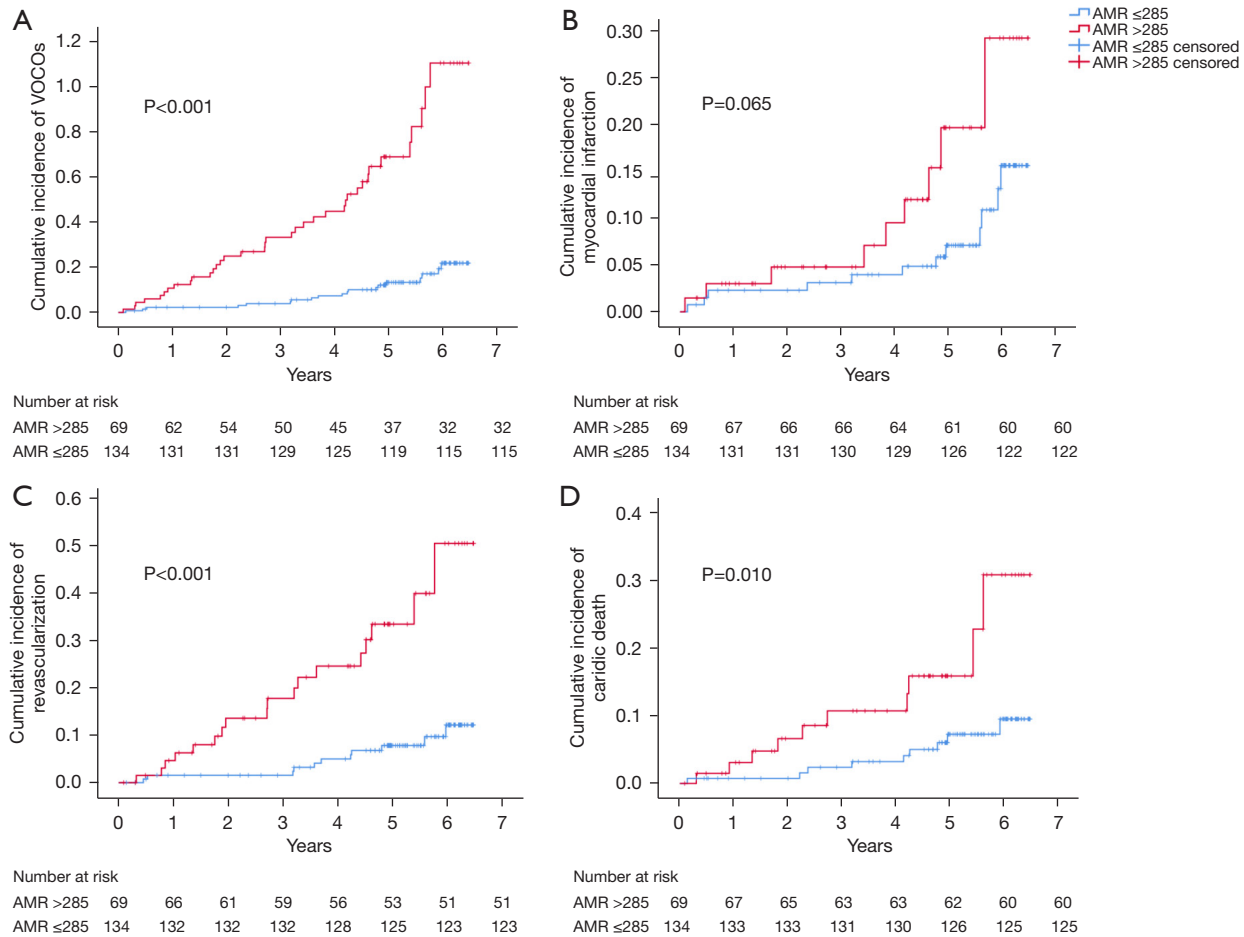

Figure 4 Cumulative incidence of VOCOs. Kaplan-Meier curves showing the cumulative incidence of VOCOs in patients with high and low AMR based on a cutoff value of 285 derived from the ROC curve. The P values were calculated with the log-rank test. When using an AMR cutoff of 285 mmHg·s/m derived from the ROC curve for predicting VOCOs, the cumulative incidence of VOCOs, myocardial infarction, revascularization, and cardiac death was significantly higher in patients with an AMR >285 mmHg·s/m (red line) than in those with an AMR of ≤285 mmHg·s/m (blue line) (P<0.001, P=0.065, P<0.001, P=0.010 respectively). AMR, angiographic microvascular resistance; VOCOs, vessel-oriented composite outcomes; ROC, receiver-operating characteristic.

consistency with wire-IMR, with an accuracy of 79.8–87.2% (9,14,15). The value of CAG-IMR for prediction of a poor prognosis has been confirmed in other studies. The Angio-IMR, developed based on the Angio-FFR, was reported to predict microcirculatory dysfunction with an optimal cutoff value of ≥25.1, with a significant association of a value greater than the cutoff with cardiovascular death and heart failure rehospitalization rates (14).

The PROSPECT study found that IVUS identified plaque burden >70%, luminal CSA area <4 mm^2, and morphology consistent with thin-cap fibrous atheroma plaque to be poor prognostic factors in the ACS population, which have been considered as partial indications for stent implantation (16). Vulnerable plaques confer a poor prognosis not only because of secondary plaque changes but also because of increased PCI-related microvascular injury. Lipid-rich plaques are more likely to experience myocardial injury after PCI. Plaque rupture under physical stress, exposure of the lipid core, embolization of plaque debris, and aggregation of inflammatory factors are associated with coronary MVD (4). Plaques identified by near-infrared spectroscopy to have lipid-rich components are more prone to periprocedural myocardial injury after PCI (4). In the present study, we identified plaque components using radiofrequency intracoronary ultrasound imaging represented by iMap-IVUS, confirming the effect of lipid

plaques on microvascular function.

In this study, we found that a higher proportion of patients with deteriorated microvascular function after PCI had ACS. Compared with chronic coronary syndrome (CCS), ACS is more likely to have microvascular dysfunction and poor prognosis due to many factors related to poor cardiac function, thrombotic lesions, and reperfusion injury, etc. (17). Cases with total occlusive lesions, thrombotic lesions, and heart failure were excluded from this study to reduce the confounding effect of other factors on microvascular function. In the study of plaque composition, iMap IVUS detected a significantly higher proportion of lipids in plaques in patients with ACS compared to those with CCS (18). The present study also found a correlation between lipidic components and microvascular dysfunction after PCI, which further validates the pathophysiological mechanisms underlying the deterioration of microvascular function and poor prognosis in ACS after PCI. According to other studies, factors such as diabetes, a high low-density lipoprotein cholesterol, and hypertension may be relevant (2,14,19) but were not found in this study. There is an association between stent over-expansion and no reflow during initial PCI for ST-segment elevation myocardial infarction (20). Another recent study has provided further insight into the degree of stent expansion and MVD (21). In that study, evaluation of the impact of different degrees of stent expansion on microvascular function and the prognosis of primary PCI QFR-based IMR found that stent over-expansion (>100%) was an independent risk factor for no reflow and major adverse cardiovascular events, whereas 70–80% of slightly under-expanded stents was not a risk factor (21). In the present study, cases with no less than 80% stent expansion were included and those with over-expansion were excluded to avoid the influence of selection bias.

Adequate preprocedural antiplatelet therapy for PCI may reduce PCI-related MVD, especially since the widespread use of ticagrelor in patients with ACS, in whom it has advantages over clopidogrel in terms of microcirculatory protection (22,23). The importance of preprocedural intravenous tirofiban has decreased but is more significant in terms of the intracoronary route (24). Intracoronary injections of agents such as sodium nitroprusside, nicorandil, adenosine, verapamil, and scopolamine can improve microcirculatory function in a short time and thus improve the prognosis, especially with regard to prevention and treatment of no reflow during primary PCI (25). Our center is accustomed to using agents such as nicorandil, nitroglycerin, and tirofiban as intracoronary agents. Considering the short-term effects of drug injection on blood flow velocity, our study did not include images after intracoronary drug injection.

This study has several limitations. First, it has a retrospective design, which means that the groups may have contained a degree of bias, and although we performed PSM to mitigate the statistical error arising from bias, the resulting decrease in sample size led to a decrease in statistical power. Second, although there is a correlation between plaque characteristics assessed by IVUS and MVD after PCI, it does not predict the prognosis, and the accuracy of detection of vulnerable thin-cap fibrous atheroma plaques is relatively weak for IVUS. Therefore, a combination of other techniques with high resolution and greater penetration, such as optical coherence tomography and near-infrared spectroscopy, are needed for more accurate identification of lesions. Third, many other factors that affect microvascular function during PCI, including degree of stent expansion, type of stent, thrombotic lesions, underlying cardiac function, medications, and other conditions, could not be analyzed because of the limitations of the study design. Fourth, the pathophysiological mechanisms of ACS and CCS are somewhat different and require further subgroup analysis. Therefore, studies that include larger samples and a more detailed study design are needed to analyze PCI-related MVD in the future. Given the limitations of this study, its results should be interpreted with caution.

In conclusion, assessment of IVUS and AMR revealed an association between smaller luminal area, more severe plaque burden, a higher percentage of lipidic components, and post-PCI MVD. Post-PCI MVD was an independent risk factor for a poor prognosis.

Acknowledgments

Funding: This work was supported by the Funds for International Cooperation and Exchange of the National Natural Science Foundation of China (No. 62161160312), Zhejiang Provincial Key Research and Development Program (No. 2020C03018), and Hangzhou Agricultural and Social Development Scientific Research Project (No. 20220919Y066).

Footnote

Conflicts of Interest: All authors have completed the ICMJE

uniform disclosure form (available at https://qims.amegroups.com/article/view/10.21037/qims-23-414/coif). JX received grants from the Hangzhou Agricultural and Social Development Scientific Research Project (No. 20220919Y066). JH received grants from Funds for International Cooperation and Exchange of the National Natural Science Foundation of China (No. 62161160312) and Zhejiang Provincial Key Research and Development Program (No. 2020C03018). The other authors have no conflicts of interest to declare.

Ethical Statement: The authors are accountable for all aspects of the work in ensuring that questions related to the accuracy or integrity of any part of the work are appropriately investigated and resolved. The study was conducted in accordance with the Declaration of Helsinki (as revised in 2013). The study was approved by ethics board of Affiliated Hangzhou First People's Hospital, Zhejiang University School of Medicine, and individual consent for this retrospective analysis was waived.

References

1. Canu M, Khouri C, Marliere S, Vautrin E, Piliero N, Ormezzano O, Bertrand B, Bouvaist H, Riou L, Djaileb L, Charlon C, Vanzetto G, Roustit M, Barone-Rochette G. Prognostic significance of severe coronary microvascular dysfunction post-PCI in patients with STEMI: A systematic review and meta-analysis. PLoS One 2022;17:e0268330.
2. Nishi T, Murai T, Ciccarelli G, Shah SV, Kobayashi Y, Derimay F, Waseda K, Moonen A, Hoshino M, Hirohata A, Yong ASC, Ng MKC, Amano T, Barbato E, Kakuta T, Fearon WF. Prognostic Value of Coronary Microvascular Function Measured Immediately After Percutaneous Coronary Intervention in Stable Coronary Artery Disease: An International Multicenter Study. Circ Cardiovasc Interv 2019;12:e007889.
3. Reffelmann T, Kloner RA. The no-reflow phenomenon: A basic mechanism of myocardial ischemia and reperfusion. Basic Res Cardiol 2006;101:359-72.
4. Stone GW, Maehara A, Muller JE, Rizik DG, Shunk KA, Ben-Yehuda O, Genereux P, Dressler O, Parvataneni R, Madden S, Shah P, Brilakis ES, Kini AS; . Plaque Characterization to Inform the Prediction and Prevention of Periprocedural Myocardial Infarction During Percutaneous Coronary Intervention: The CANARY Trial (Coronary Assessment by Near-infrared of Atherosclerotic Rupture-prone Yellow). JACC Cardiovasc Interv 2015;8:927-36.
5. Xu B, Tu S, Qiao S, Qu X, Chen Y, Yang J, Guo L, Sun Z, Li Z, Tian F, Fang W, Chen J, Li W, Guan C, Holm NR, Wijns W, Hu S. Diagnostic Accuracy of Angiography-Based Quantitative Flow Ratio Measurements for Online Assessment of Coronary Stenosis. J Am Coll Cardiol 2017;70:3077-87.
6. Ai H, Feng Y, Gong Y, Zheng B, Jin Q, Zhang HP, Sun F, Li J, Chen Y, Huo Y, Huo Y. Coronary Angiography-Derived Index of Microvascular Resistance. Front Physiol 2020;11:605356.
7. De Maria GL, Scarsini R, Shanmuganathan M, Kotronias RA, Terentes-Printzios D, Borlotti A, Langrish JP, Lucking AJ, Choudhury RP, Kharbanda R, Ferreira VM; Channon KM, Garcia-Garcia HM, Banning AP. Angiography-derived index of microcirculatory resistance as a novel, pressure-wire-free tool to assess coronary microcirculation in ST elevation myocardial infarction. Int J Cardiovasc Imaging 2020;36:1395-406.
8. Scarsini R, Shanmuganathan M, Kotronias RA, Terentes-Printzios D, Borlotti A, Langrish JP, Lucking AJ; Ribichini F, Ferreira VM, Channon KM, Garcia-Garcia HM, Banning AP, De Maria GL. Angiography-derived index of microcirculatory resistance (IMR(angio)) as a novel pressure-wire-free tool to assess coronary microvascular dysfunction in acute coronary syndromes and stable coronary artery disease. Int J Cardiovasc Imaging 2021;37:1801-13.
9. Fan Y, Fezzi S, Sun P, Ding N, Li X, Hu X, Wang S, Wijns W, Lu Z, Tu S. In Vivo Validation of a Novel Computational Approach to Assess Microcirculatory Resistance Based on a Single Angiographic View. J Pers Med 2022;12:1798.
10. De Maria GL, Cuculi F, Patel N, Dawkins S, Fahrni G, Kassimis G, Choudhury RP, Forfar JC, Prendergast BD, Channon KM, Kharbanda RK, Banning AP. How does coronary stent implantation impact on the status of the

microcirculation during primary percutaneous coronary intervention in patients with ST-elevation myocardial infarction? Eur Heart J 2015;36:3165-77.
11. Wang W, Hu Y, Xiang P, Sheng X, Leng X, Yang X, Dong L, Li C, Sun Y, Jiang J, Xiang J, Lin X. The diagnostic performance of AccuFFRangio for evaluating coronary artery stenosis under different computational conditions. Quant Imaging Med Surg 2023;13:2496-506.
12. Xu B, Tu S, Song L, Jin Z, Yu B, Fu G, et al. Angiographic quantitative flow ratio-guided coronary intervention (FAVOR III China): a multicentre, randomised, sham-controlled trial. Lancet 2021;398:2149-59.
13. Song L, Xu B, Tu S, Guan C, Jin Z, Yu B, et al. 2-Year Outcomes of Angiographic Quantitative Flow Ratio-Guided Coronary Interventions. J Am Coll Cardiol 2022;80:2089-101.
14. Dai N, Che W, Liu L, Zhang W, Yin G, Xu B, Xu Y, Duan S, Yu H, Li C, Yao K, Huang D, Ge J. Diagnostic Value of Angiography-Derived IMR for Coronary Microcirculation and Its Prognostic Implication After PCI. Front Cardiovasc Med 2021;8:735743.
15. Tebaldi M, Biscaglia S, Di Girolamo D, Erriquez A, Penzo C, Tumscitz C, Campo G. Angio-Based Index of Microcirculatory Resistance for the Assessment of the Coronary Resistance: A Proof of Concept Study. J Interv Cardiol 2020;2020:8887369.
16. Stone GW, Maehara A, Lansky AJ, de Bruyne B, Cristea E, Mintz GS, Mehran R, McPherson J, Farhat N, Marso SP, Parise H, Templin B, White R, Zhang Z, Serruys PW; . A prospective natural-history study of coronary atherosclerosis. N Engl J Med 2011;364:226-35.
17. Lerman A, Holmes DR, Herrmann J, Gersh BJ. Microcirculatory dysfunction in ST-elevation myocardial infarction: cause, consequence, or both? Eur Heart J 2007;28:788-97.
18. Kozuki A, Shinke T, Otake H, Shite J, Matsumoto D, Kawamori H, Nakagawa M, Nagoshi R, Hariki H, Inoue T, Nishio R, Hirata K. Feasibility of a novel radiofrequency signal analysis for in-vivo plaque characterization in humans: comparison of plaque components between patients with and without acute coronary syndrome. Int J Cardiol 2013;167:1591-6.
19. Fearon WF, Low AF, Yong AS, McGeoch R, Berry C, Shah MG, Ho MY, Kim HS, Loh JP, Oldroyd KG. Prognostic value of the Index of Microcirculatory Resistance measured after primary percutaneous coronary intervention. Circulation 2013;127:2436-41.
20. Maekawa Y, Asakura Y, Anzai T, Ishikawa S, Okabe T, Yoshikawa T, Ogawa S. Relation of stent overexpansion to the angiographic no-reflow phenomenon in intravascular ultrasound-guided stent implantation for acute myocardial infarction. Heart Vessels 2005;20:13-8.
21. Li X, Sun S, Luo D, Yang X, Ye J, Guo X, Xu S, Sun B, Zhang Y, Luo J, Zhou Y, Tu S, Dong H. Microvascular and Prognostic Effect in Lesions With Different Stent Expansion During Primary PCI for STEMI: Insights From Coronary Physiology and Intravascular Ultrasound. Front Cardiovasc Med 2022;9:816387.
22. Park SD, Lee MJ, Baek YS, Kwon SW, Shin SH, Woo SI, Kim DH, Kwan J, Park KS. Randomised trial to compare a protective effect of Clopidogrel Versus TIcagrelor on coronary Microvascular injury in ST-segment Elevation myocardial infarction (CV-TIME trial). EuroIntervention 2016;12:e964-71.
23. Firman D, Taslim I, Wangi SB, Yonas E, Pranata R, Alkatiri AA. The effect of early dual antiplatelet timing on the microvascular resistance and ventricular function in primary percutaneous coronary intervention. Medicine (Baltimore) 2020;99:e21177.
24. Ma Q, Ma Y, Wang X, Li S, Yu T, Duan W, Wu J, Wen Z, Jiao Y, Sun Z, Hou Y. Intracoronary compared with intravenous bolus tirofiban on the microvascular obstruction in patients with STEMI undergoing PCI: a cardiac MR study. Int J Cardiovasc Imaging 2020;36:1121-32.
25. Niu X, Zhang J, Bai M, Peng Y, Sun S, Zhang Z. Effect of intracoronary agents on the no-reflow phenomenon during primary percutaneous coronary intervention in patients with ST-elevation myocardial infarction: a network meta-analysis. BMC Cardiovasc Disord 2018;18:3.

Cite this article as: Xie J, He Y, Ji H, Hu Q, Chen S, Gao B, Yang J, Jin X, Zhou L, Wang N, Tong X, Tong G, Huang J. Impact of plaque characteristics on percutaneous coronary intervention-related microvascular dysfunction: insights from angiographic microvascular resistance and intravascular ultrasound. Quant Imaging Med Surg 2023;13(9):6037-6047. doi: 10.21037/qims-23-414

